scientific reports

Check for updates

OPEN

A mitochondrial metalloprotease FtsH4 is required for symbiotic nitrogen fixation in *Lotus japonicus* nodules

Yoshikazu Shimoda[1,10]✉, Hiroko Yamaya-Ito[1,5,10], Tsuneo Hakoyama[1,6], Shusei Sato[2,7], Takakazu Kaneko[2,8], Satoshi Shibata[1,9], Masayoshi Kawaguchi[3], Norio Suganuma[4], Makoto Hayashi[1,6], Hiroshi Kouchi[1] & Yosuke Umehara[1]✉

Symbiotic nitrogen fixation is a highly coordinated process involving legume plants and nitrogen-fixing bacteria known as rhizobia. In this study, we investigated a novel Fix⁻ mutant of the model legume *Lotus japonicus* that develops root nodules with endosymbiotic rhizobia but fails in nitrogen fixation. Map-based cloning identified the causal gene encoding the filamentation temperature-sensitive H (FtsH) protein, designated as *LjFtsH4*. The *LjFtsH4* gene was expressed in all plant organs without increased levels during nodulation. Subcellular localization revealed that LjFtsH4, fused with a fluorescent protein, localized in mitochondria. The *Ljftsh4* mutant nodules showed signs of premature senescence, including symbiosome membrane collapse and bacteroid disintegration. Additionally, nodule cells of *Ljftsh4* mutant displayed mitochondria with indistinct crista structures. Grafting and complementation tests confirmed that the Fix⁻ phenotype was determined by the root genotype, and that protease activity of LjFtsH4 was essential for nodule nitrogen fixation. Furthermore, the ATP content in *Ljftsh4* mutant roots and nodules was lower than in the wild-type, suggesting reduced mitochondrial function. These findings underscore the critical role of LjFtsH4 in effective symbiotic nitrogen fixation in root nodules.

Keywords Nodule symbiosis, Symbiotic nitrogen fixation, ATP-dependent metalloprotease, Mitochondrial dysfunction

Symbiotic nitrogen fixation by legume root nodules is a vital biological process that significantly contributes to nitrogen uptake in terrestrial ecosystems and crop production in agricultural lands. This process involves the infection of host plant roots by symbiotic rhizobia, the development of root nodules, and the subsequent nitrogen fixation by rhizobia within these nodules. These processes are tightly regulated by both the host legume and the symbiotic rhizobia.

Rhizobial infection begins with the mutual recognition of symbiotic signals from both partners. Host root-secreted flavonoids are perceived by symbiotic rhizobia, inducing the production of lipochito-oligosaccharide signals known as Nod factors (NFs). Host plant receptors containing Lysine-motif (LysM) in their extracellular domain then recognize these rhizobial NFs. In model legumes like *Lotus japonicus* and *Medicago truncatula*, a complex of LysM receptors (NFR1 and NFR5 in *L. japonicus*, LYK3 and NFP in *M. truncatula*) are responsible for recognizing compatible NFs[1–3]. This recognition triggers calcium (Ca^{2+}) oscillation, known as Ca^{2+} spiking, in the nucleus of host root cells[4]. NF perception and Ca^{2+} spiking are mediated by leucine-rich repeat receptor

[1]Institute of Agrobiological Sciences, National Agriculture and Food Research Organization, Tsukuba, Ibaraki 305-8604, Japan. [2]Kazusa DNA Research Institute, Kisarazu, Chiba 292-0818, Japan. [3]National Institute for Basic Biology, Okazaki, Aichi 444-8585, Japan. [4]Department of Life Science, Aichi University of Education, Kariya, Aichi 448-8542, Japan. [5]Present address: College of Bioresource Sciences, Nihon University, Fujisawa, Kanagawa 252-0880, Japan. [6]Present address: Center for Sustainable Resource Science, RIKEN, Yokohama, Kanagawa 230-0045, Japan. [7]Present address: Graduate School of Life Sciences, Tohoku University, Sendai, Miyagi 980-8577, Japan. [8]Present address: Faculty of Life Sciences, Kyoto Sangyo University, Kita-ku, Kyoto 603-8555, Japan. [9]Present address: Mining and Metallurgy Laboratories Technology Development Department, Metals Company, Mitsubishi Materials Corporation, Iwaki, Fukushima 971-8101, Japan. [10]These authors contributed equally to this work: Yoshikazu Shimoda and Hiroko Yamaya-Ito. ✉email: yshimoda@affrc.go.jp; umehara@affrc.go.jp

kinases SYMRK/DMI2 and several receptor-interacting proteins[4]. Studies on symbiotic mutants defective in Ca^{2+} spiking have revealed several nuclear proteins involved in generating the calcium signals. These proteins include cation channels, LjCASTOR and LjPOLLUX/MtDMI1[5,6], MtCNGC[7], calcium ATPase MCA8[8], and nucleoporins (LjNUP133, LjNUP85, LjNENA)[9–11]. Calcium and calmodulin-dependent protein kinase (CCaMK) decodes the nuclear Ca^{2+} signals to induce downstream symbiotic genes for rhizobial infection and cortical cell division, leading to nodule organogenesis[12,13]. CYCLOPS (IPD3) is a transcription factor that transmits the Ca^{2+} signals decoded by CCaMK and induces downstream gene expression[14,15]. Nodule inception (NIN) is induced exclusively in response to NF and is crucial for both rhizobial infection and nodule organogenesis[16]. Ectopic expression of *NIN* induces nodule development in cooperation with other transcription factors, such as nuclear factor Y (NF-Y) and ASL18/LBD16[16,17]. Through these signalling cascades, infection by symbiotic rhizobia ultimately leads to the development of specialized organs, root nodules, where the rhizobia reside and fix atmospheric nitrogen.

Nitrogen fixation within nodules is conducted by the rhizobial enzyme nitrogenase, which is, in most cases, induced only in the bacteroids, the symbiotic form of rhizobia in nodules. Identification of a number of legume Fix^- mutants, which develop root nodules with endosymbiotic rhizobia but are impaired in nitrogen fixation, indicates the existence of host legume genes that control rhizobial nitrogen fixation activity. The Fix^- genes identified so far can be classified into three categories based on their function within the nodule. The first category comprises genes encoding enzymes and proteins for nodule-specific metabolism required for the expression and maintenance of bacteroid nitrogenase activity. This category includes the homocitrate synthase FEN1[18], which provides the bacteroid with homocitrate, an essential component of the Fe-Mo cofactor of nitrogenase. Reverse-genetic approaches have also revealed nodule-specific or nodule-upregulated host plant genes/proteins that can be classified into the first category. These include genes for leghaemoglobins[19], sucrose synthase[20], and phosphoenolpyruvate carboxylase[21]. The second category includes genes involved in the transport of metabolites between plant cells and bacteroids. SST1, a nodule-specific sulfate transporter that mediates the supply of sulfate[22], and SEN1, a molybdate transporter in nodule-infected cells[23], can be classified in this category. Additionally, other transporters in nodules, such as those for iron, citrate, dicarboxylate, and ammonium, are also involved in nodule nitrogen fixation[24]. The third category comprises genes required for bacteroid differentiation or nodule immunity. Legumes belonging to the inverted-repeat lacking clade (IRLC), such as *Medicago* and pea, express hundreds of genes for nodule-specific cysteine-rich (NCR) peptides[25], which play pivotal roles in bacteroid differentiation. The loss of specific NCR peptides results in Fix^- phenotypes in *M. truncatula*[26,27]. Several genes that control nodule immunity were identified from Fix^- mutants of *M. truncatula*, including the genes for DNF2, SymCRK, RSD, and NAD1[28]. Mutations in these genes lead to the development of nodules with increased defense responses, indicating that these gene products act as defense repressors in nodules.

Although extensive studies have been conducted, our understanding of the host plant factors responsible for regulating symbiotic nitrogen fixation activity remains limited. In this study, we characterized a novel symbiotic mutant of *L. japonicus* impaired in symbiotic nitrogen fixation. Map-based cloning revealed that the causal gene encodes the membrane-bound, ATP-dependent metalloprotease, known as Filamentation temperature-sensitive H (FtsH) protease[29]. We designated the mutant as *Ljftsh4*. In root nodule symbiosis, several host plant proteases (peptidases) regulate nitrogen fixation activity. Cysteine proteases are abundantly expressed in old or stressed nodules, some of which are involved in nodule senescence[30–32]. We have previously shown that APN1, a nodule-specific aspartic peptidase of *L. japonicus*, determines the compatibility of symbiotic nitrogen fixation with specific rhizobial strains[33,34]. DNF1 of *M. truncatula* encodes a signal peptidase required for the maturation of NCR peptides by cleaving the N-terminal signal peptide[35,36]. Rhizobial peptidases also play an important role in regulating symbiotic nitrogen fixation. *Sinorhizobium meliloti* metallopeptidase (HrrP) is involved in cleaving host-encoded NCR peptides and promoting the proliferation of rhizobia in nodules[37]. This study is the first to demonstrate the importance of the host plant ATP-dependent metalloprotease for effective symbiotic nitrogen fixation in legume root nodules.

Results

Symbiotic phenotypes of the *Ljftsh4* mutant

The *Ljftsh4-1* mutant (formerly known as *sym102* in Sandal et al.[38]) was isolated from the progeny of regenerated plants from calli derived from *L. japonicus* B-129 Gifu. When grown under nitrogen-free conditions and inoculated with symbiotic rhizobia *Mesorhizobium loti*, the *Ljftsh4-1* mutant exhibited stunted shoot growth compared to the wild-type plant (Fig. 1a). The nodules formed on the *Ljftsh4-1* mutant were white to pale green, in contrast to the pink nodules formed on the wild-type (Fig. 1a). The total nodule numbers in the *Ljftsh4-1* mutant at 21 and 28 days after inoculation (dai) were slightly higher than those of the wild-type (Fig. 1b). At 14 and 21 dai, the *Ljftsh4-1* mutant very rarely formed nodules with a pale pink colour (Fig. 1c). Nitrogen fixation activity, as estimated by acetylene reduction activity (ARA), was significantly lower in the mutant compared to the wild-type (Fig. 1d, e). The exogenous application of potassium nitrate (KNO_3) to the *Ljftsh4-1* mutant promoted shoot and root growth but did not fully restore growth to the levels observed in the wild-type plant (Supplemental Fig. 1).

At 16 dai, light microscopy of nodule sections from the *Ljftsh4-1* mutant showed the presence of rhizobia in infected cells, but the toluidine blue staining was less intense than in the wild-type (Fig. 2a, b). Large vacuoles found in wild-type nodules were not observed in most of the infected cells of the *Ljftsh4-1* mutant (Fig. 2c, d). Transmission electron microscopy revealed that in wild-type nodules, bacteroids appeared to be surrounded by a clear symbiosome membrane (Fig. 2e, g), whereas the symbiosome membrane was indistinct in the *Ljftsh4-1* nodules (Fig. 2f, h). Additionally, some starch granules were observed in the *Ljftsh4-1* nodules (Fig. 2f). These

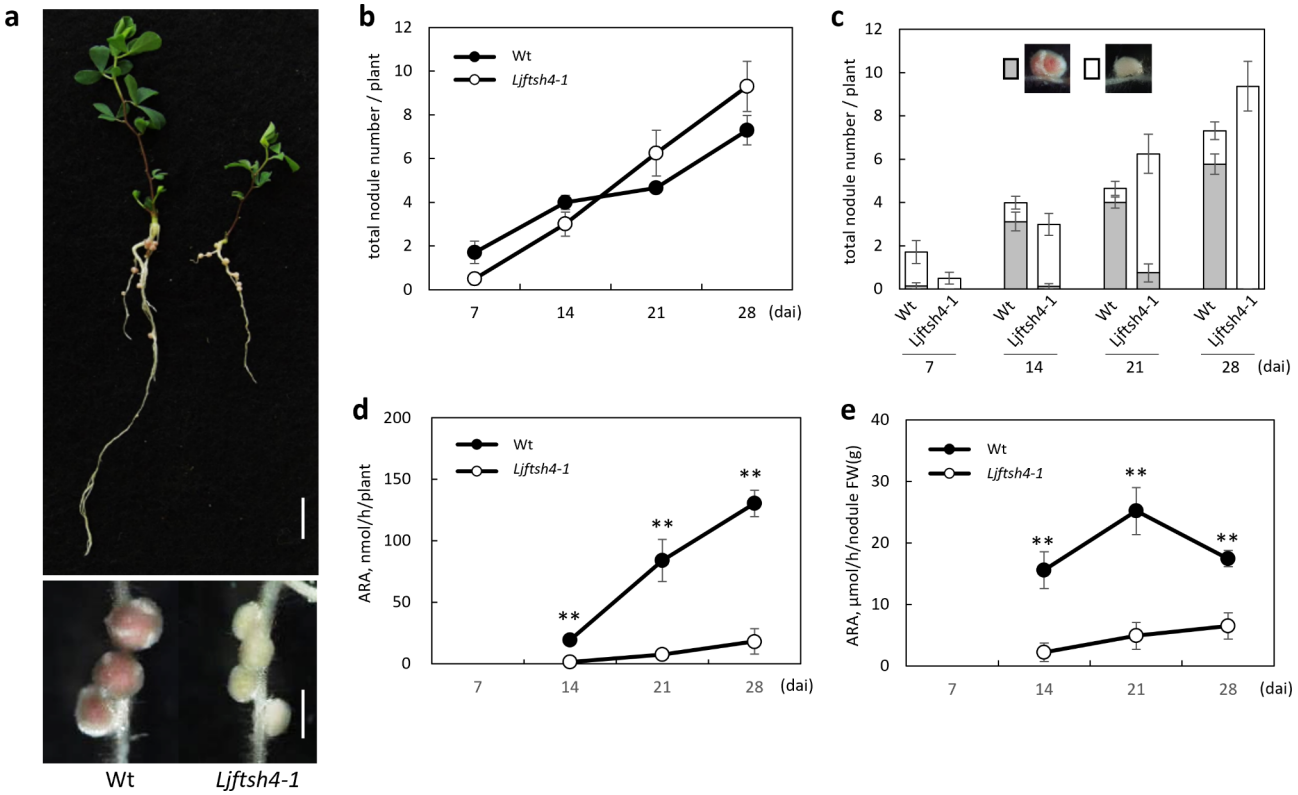

Fig. 1. Symbiotic phenotypes of the *Ljftsh4-1* mutant. (**a**) Plant growth (upper panel) and nodulation phenotype (lower panel) of the wild-type (Wt) B-129 Gifu (left) and the *Ljftsh4-1* mutant (right) inoculated with *M. loti*. Pictures were taken 28 days after *M. loti* inoculation. Scale bars: 1 cm (upper panel), 1 mm (lower panel). (**b**) Total number of nodules per plant and (**c**) number of mature pink nodules (grey bars) and Fix^- nodules (white bars). Values are means with standard error of eight plants. Inset photos in (**c**) show typical pink mature and Fix^- nodules, respectively. (**d, e**) Acetylene reduction activity (ARA) per plant (**d**) and per nodule fresh weight (**e**). Values are means with standard error of 12 plants. ** indicates a significant difference at $P < 0.01$ (Student's *t*-test).

phenotypes suggest that premature nodule senescence, characterized by the collapse of the symbiosome membrane and disintegration of bacteroids, occurs in the *Ljftsh4-1* mutant nodules.

Map-based cloning of the *LjFtsH4* gene

To identify the causal gene of the *Ljftsh4-1* mutant, we conducted map-based cloning using *L. japonicus* MG-20[39] as a crossing partner. The *LjFtsH4* locus was positioned on chromosome 1 between the simple sequence repeat (SSR) markers TM0671 and TM0349 (Supplemental Fig. 2a). Fine mapping with 1,644 F2 progeny narrowed down the *LjFtsH4* locus to a 180-kb region between the markers BM2176 and TM0349. The genome sequence of *L. japonicus* build 2.5[40] contains twenty-six putative open reading frames (ORFs) in this region (Supplemental Fig. 2a). Comparison of the genome sequences of these ORFs in both the wild-type and the *Ljftsh4-1* mutant revealed a 784 bp deletion in the 7th ORF of the *Ljftsh4-1* mutant genome, resulting in a premature stop codon. Re-annotation of the genome sequence revealed that the 7th and 9th ORFs correspond to a single gene, *Lj1g3v1786070* (*L. japonicus* genome sequence build 3.0), and a retrotransposon-like sequence, predicted as the 8th ORF, is inserted between the two ORFs (Supplemental Fig. 2a, b). *LjFtsH4* gene is approximately 10 kbp long and consists of seven exons, with the mutation located in the 7th exon (Supplemental Fig. 2b).

LjFtsH4 encodes an ATP-dependent metalloprotease that belongs to the FtsH family of peptidases[29]. Functional domain analysis using InterProScan[41] revealed that LjFtsH4 contains AAA (ATPases Associated with Diverse Cellular Activities) (PF00004), AAA_lid_3 (PF17862), and peptidase M41 (PF01434) domains (Fig. 3a). The *Ljftsh4-1* mutant, obtained from regenerated plants (G00496-9-6), contains a mutation in the peptidase M41 domain (Supplemental Fig. 2c). We isolated four additional mutant alleles through C_6^+ ion beam or ethyl methanesulphonate (EMS) mutagenesis on *L. japonicus* ecotype MG-20 (Supplemental Fig. 2d). All these mutants contain mutations within the peptidase M41 domain (Supplemental Fig. 2c, d). Similar to the *Ljftsh4-1* mutant, mutant alleles derived from ecotype MG-20 (*Ljftsh4-2* to *Ljftsh4-5*) exhibited stunted plant growth compared to the wild-type and formed white nodules when inoculated with symbiotic rhizobia (Supplemental Fig. 3a, b). The growth of the *Ljftsh4* mutant alleles was promoted by the addition of exogenous nitrogen nutrient (KNO_3) but was not fully restored to the level of the wild-type plant (Supplemental Fig. 4).

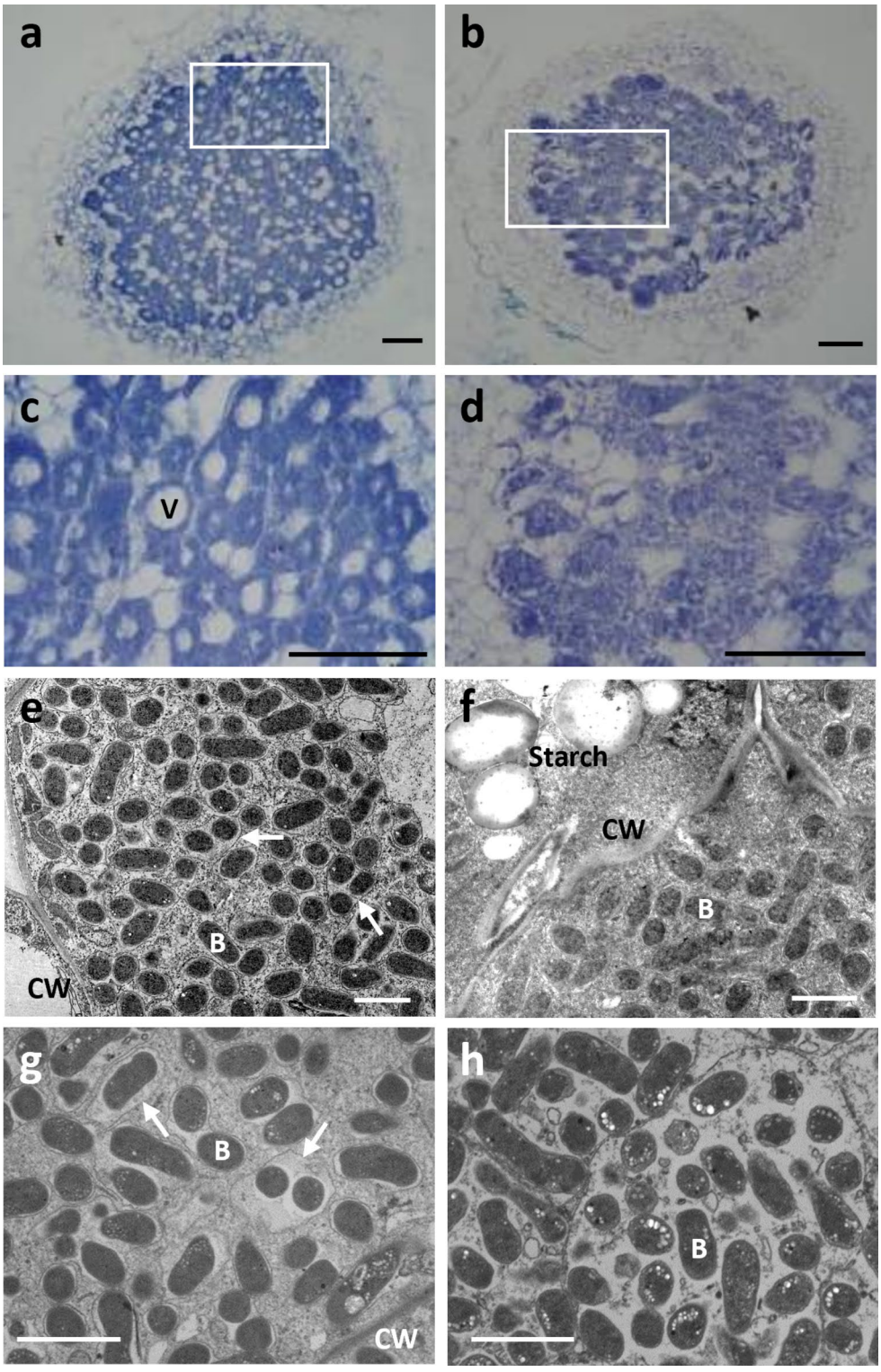

Fig. 2. Structure of the *Ljftsh4-1* mutant nodule cells. (**a**-**d**) Optical micrographs of nodule sections from the wild-type (**a, c**) and the *Ljftsh4-1* mutant (**b, d**) at 16 days after inoculation (dai). (**c, d**) are magnified images of the boxed areas in (**a, b**), respectively. Vacuole (V) in the wild-type nodule infected cell is shown in (**c**). Scale bars: 100 µm (**a, b**) and 25 µm (**c, d**). (**e**-**h**) Electron micrographs of nodule sections from the wild-type (**e, g**) and the *Ljftsh4-1* mutant (**f, h**) at 11 dai (**e, f**) and 18 dai (**g, h**). B, bacteroid; CW, cell wall. Starch granule accumulation is observed in the *Ljftsh4-1* nodule (starch in **f**). Arrows in (**e**) and (**g**) indicate the peribacteroid membrane. Scale bars: 2 µm.

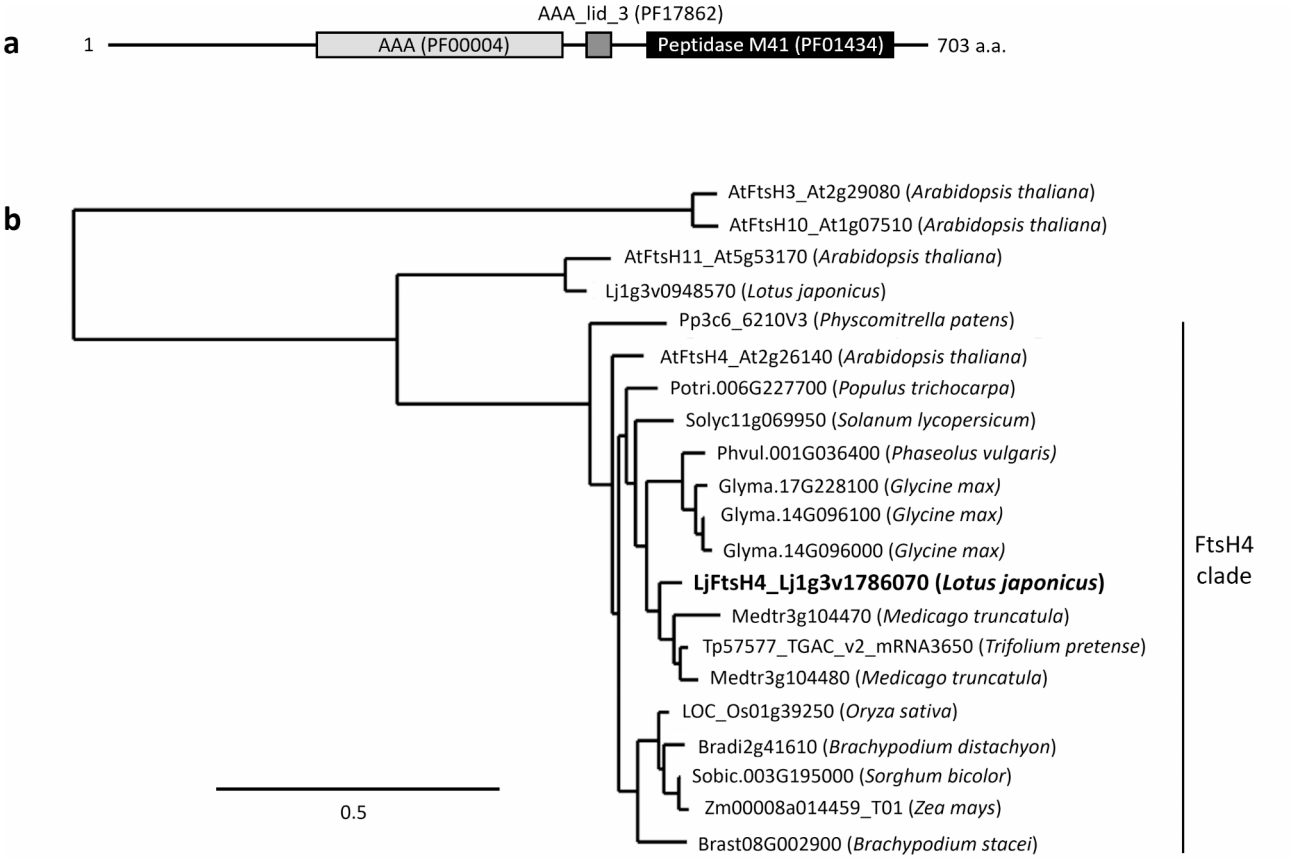

Fig. 3. Protein structure of LjFtsH4 and phylogenetic tree of plant FtsH proteins. (**a**) Protein structure of LjFtsH4 consisting of the ATPase family associated with various cellular activities (AAA) (PF00004), AAA_lid_3 domain (PF17862), and Peptidase M41 (PF01434) domain as predicted by Pfam. (**b**) Phylogenetic tree of plant FtsH4 proteins. Gene IDs are followed by plant species in parentheses. LjFtsH4 of *L. japonicus* is shown in bold. AtFtsH3 and AtFtsH10 are used as outgroup.

LjFtsH4 shares structural similarities with YME1 of yeast[42] and FtsH4 of *Arabidopsis*[43]. Phylogenetic analysis shows that LjFtsH4 belongs to the FtsH4 group and is located in the clade that includes FtsH4 homologs of legumes (Fig. 3b). The closest paralogous gene of *L. japonicus* (*Lj1g3v0948570*) clusters with *Arabidopsis* FtsH11 (*At5g53170*), which is another AAA protease with a different function from AtFtsH4[44].

The *LjFtsH4* gene is expressed in aerial parts (leaves, flowers, stems, pods, and flower buds), as well as in roots and nodules. The expression levels did not change significantly during nodule development (Fig. 4). Constitutive expression throughout the plant organs and during nodule development is also observed in the orthologous genes of *M. truncatula* (*Medtr3g104470* and *Medtr3g104480*), as examined by the Gene Expression Atlas[45].

Complementation assay of the *Ljftsh4* mutant

To confirm that the gene *Lj1g3v1786070* identified from map-based cloning is the causal gene of the *Ljftsh4* mutant, a complementation test was conducted using hairy root transformation. *Ljftsh4-1* plants with hairy roots transformed with polyubiquitin promoter (pUbi)::*LjFtsH4* cDNA formed numerous pink, mature nodules and exhibited improved shoot growth. In contrast, control plants transformed with an empty vector produced white nodules and showed poor growth (Fig. 5a). The nitrogen fixation activity of nodules on roots transformed with *LjFtsH4* cDNA was significantly higher than that of the empty vector controls (Fig. 5b), comparable to that in the wild-type (Fig. 1e), confirming that *Lj1g3v1786070* is indeed the causal gene of the *Ljftsh4-1* mutant.

Since LjFtsH4 is an ortholog of the *Arabidopsis* FtsH4 (AtFtsH4), we also performed complementation analysis using *AtFtsH4* cDNA. This analysis showed that *AtFtsH4* successfully complemented the *Ljftsh4-1* mutant, resulting in the formation of mature pink nodules with nitrogen fixation activity comparable to those on *LjFtsH4*-transformed roots (Fig. 5a, b). As reported for AtFtsH4[43], *LjFtsH4* did not complement the yeast *yme1* mutant, suggesting a different function from yeast YME1 (Supplemental Fig. 5).

To determine whether the protease activity of LjFtsH4 is necessary for its role in symbiotic nitrogen fixation, we conducted further complementation analyses using mutated LjFtsH4 variants. Mutations that would eliminate the protease activity of LjFtsH4 were introduced, based on mutagenesis information from *E. coli* FtsH proteins, as there is limited information on loss-of-function mutations for plant and yeast FtsH4 proteases. In the AAA domain of *E. coli* FtsH (UniProtID: P0AAI3), mutations in Arg309 and Arg312 cause a loss of ATPase activity in vitro[46]. Additionally, mutations in the zinc-binding site (414-HEGEH-418) result in a loss of protease

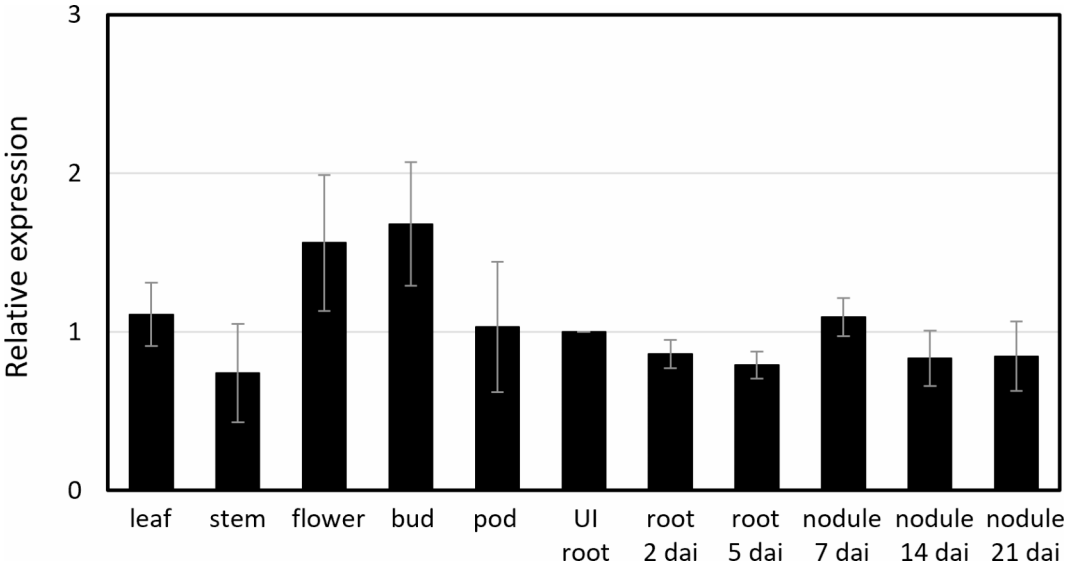

Fig. 4. Expression profiles of *LjFtsH4* gene in different organs. Bars represent the means of three independent experiments with standard error and are shown as relative expression to the level in uninoculated (UI) roots, which is set to 1. All values were normalized against the expression of the *L. japonicus* ubiquitin gene (Flemetakis et al.[88]) as an internal standard. No significant differences in *LjFtsH4* expression were observed between roots and other organs. dai indicates days after inoculation with rhizobia.

activity[46,47]. These amino acid residues are conserved among yeast and plant FtsH4 proteins, and we introduced the same mutations at the corresponding residues in LjFtsH4 (Supplemental Fig. 6a). Transformation with the mutated LjFtsH4 (R378A_R381A and H483Y_E484Q_H487Y) did not restore the formation of mature pink nodules in the *Ljftsh4-1* mutant (Supplemental Fig. 6b). This indicates that the protease activity of LjFtsH4 is essential for its function in symbiotic nitrogen fixation in nodules.

Grafting experiment of *Ljftsh4* mutant

The *LjFtsH4* gene is constitutively expressed throughout the plant organs (Fig. 4), indicating that the gene might control nitrogen fixation in nodules systemically. To determine whether above- or below-ground mutations are responsible for the Fix$^-$ phenotypes of the *Ljftsh4* mutant, we conducted a grafting experiment. When the *Ljftsh4-1* shoot was grafted onto wild-type roots, mature pink nodules with nitrogen fixation activity were formed, with activity levels comparable to those of the wild-type control (wild-type shoot/wild-type root). In contrast, when the wild-type shoot was grafted onto *Ljftsh4-1* roots, both plant weight and nitrogen fixation activity were as low as those of the mutant control (*Ljftsh4-1* shoot/*Ljftsh4-1* root) (Supplemental Fig. 7). These results indicate that the Fix$^-$ phenotypes of the *Ljftsh4-1* mutant is determined by the root genotype.

Subcellular localization of LjFtsH4 protein

Plant FtsH4 is reported as a mitochondrial protein[43,48,49]. Indeed, prediction using TargetP[50] and MultiLOC[51] programs indicated that the LjFtsH4 protein likely localizes to mitochondria, similar to *Arabidopsis* FtsH4[43]. To verify the subcellular localization of the LjFtsH4 protein, we constructed a fusion protein of green fluorescent protein (GFP) and LjFtsH4. GFP was translationally fused at the C-terminal end of LjFtsH4, and the resulting LjFtsH4-GFP was expressed using the polyubiquitin promoter of *L. japonicus*[52]. As a mitochondrial localization marker, we used the gamma subunit of mitochondrial F1-ATPase (pFAγ, AT2G33040) from *Arabidopsis*[53]. The N-terminal 72 amino acids of pFAγ were fused to red fluorescent protein (RFP) at its N-terminal end, and pFAγ-RFP was also expressed using the *L. japonicus* polyubiquitin promoter. When both LjFtsH4-GFP and pFAγ-RFP were co-expressed in the hairy roots, punctate GFP signals were observed. These signals co-localized with the RFP signals of the mitochondrial marker (Fig. 6), confirming that LjFtsH4 localizes to mitochondria.

To determine whether the mutation in the *Ljftsh4* gene affects the distribution and appearance of mitochondria, we compared the distribution of the mitochondrial marker (pFAγ-RFP) between wild-type and *Ljftsh4-1* mutant cells. In root cells, the distribution and number of RFP signals were similar in both wild-type and *Ljftsh4-1* mutant cells, regardless of nutrient conditions (Supplemental Fig. 8a, b). These results suggest that the mutation in the *Ljftsh4* gene does not significantly affect the distribution of root mitochondria. In nodules, however, the distribution of the mitochondrial marker differed between wild-type and *Ljftsh4-1* mutant cells. In wild-type nodule cells, punctate RFP signals were found along the cell outlines, whereas in *Ljftsh4-1* mutant cells, the signals were less distinct and dispersed throughout the cells (Supplemental Fig. 8c).

Transmission electron microscopy (TEM) of nodules revealed morphological differences in mitochondria between wild-type and *Ljftsh4* mutants. In wild-type nodule cells, mitochondrial cristae, folds in the inner membrane of mitochondria[54], were clearly observed, while in *Ljftsh4* mutants, the cristae were not distinct (Fig. 7a, b).

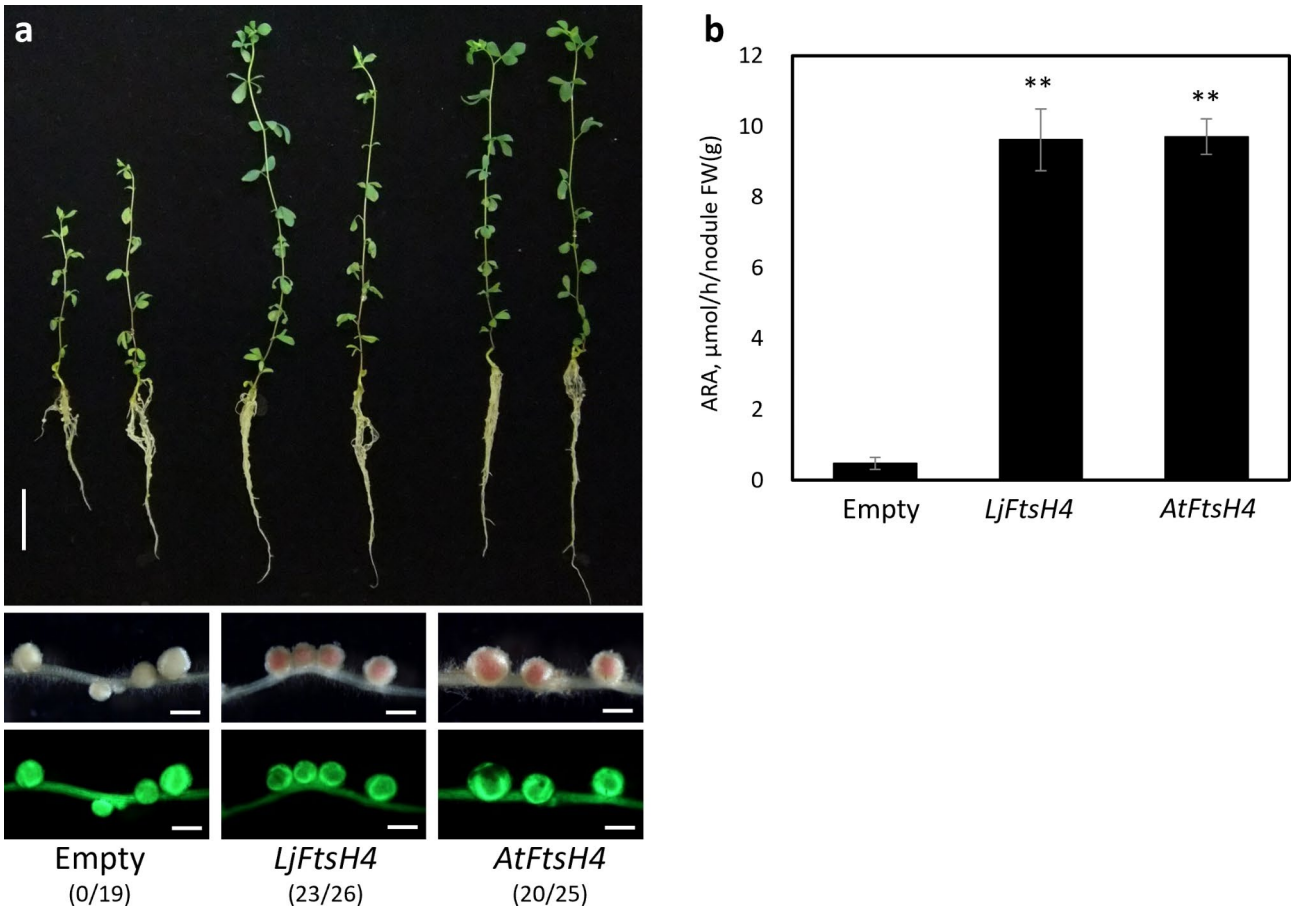

Fig. 5. Complementation assay of the *Ljftsh4-1* mutant. (**a**) Complementation of the *Ljftsh4-1* mutant with *LjFtsH4* and *AtFtsH4* cDNAs. Plant growth phenotype (upper panel) and nodules formed on transformed hairy roots expressing GFP as a transformation marker (lower panel). Pictures were taken 28 days after rhizobial inoculation. Scale bars: 2 cm (upper panel) and 1 mm (lower panel). Empty indicates complementation with the empty vector. Numbers in parentheses indicate the number of plants that formed nitrogen-fixing nodules out of the total number of plants analysed. (**b**) Acetylene reduction activity of nodules formed on transformed roots at 28 days after rhizobial inoculation. Values are means with standard error of 6 independent transformants. ** indicates significant differences ($P < 0.01$) compared to the empty vector (Student's *t*-test).

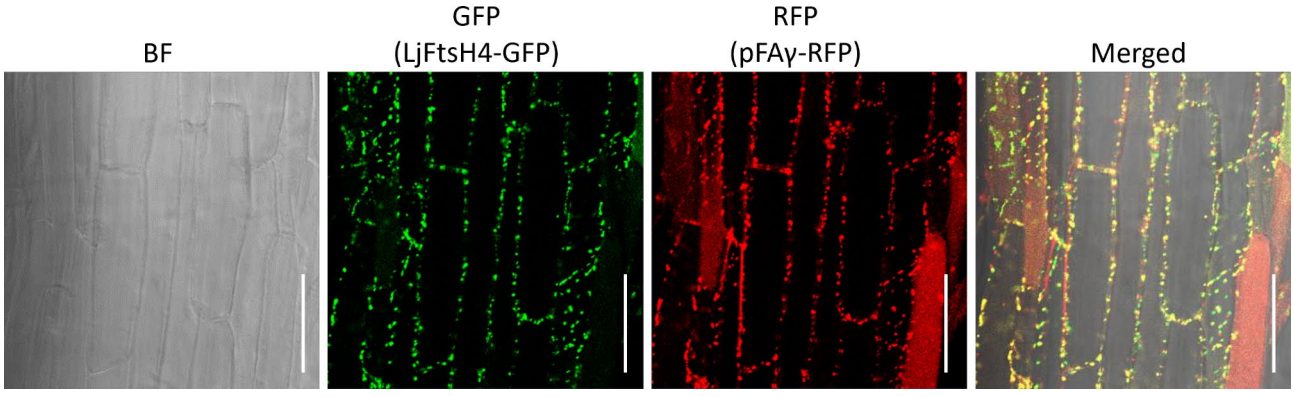

Fig. 6. Subcellular localization of LjFtsH4. Confocal microscope images showing the mitochondrial localization of the GFP-fused LjFtsH4 (LjFtsH4-GFP) in root epidermis. pFAγ-RFP (RFP-fused N-terminal part of the gamma subunit of mitochondrial F1-ATPase of *Arabidopsis*) is a marker for mitochondrial localization. LjFtsH4-GFP co-localized with pFAγ-RFP, as shown in merged images of GFP and RFP (Merged). BF is a bright field image. Scale bars = 50 µm.

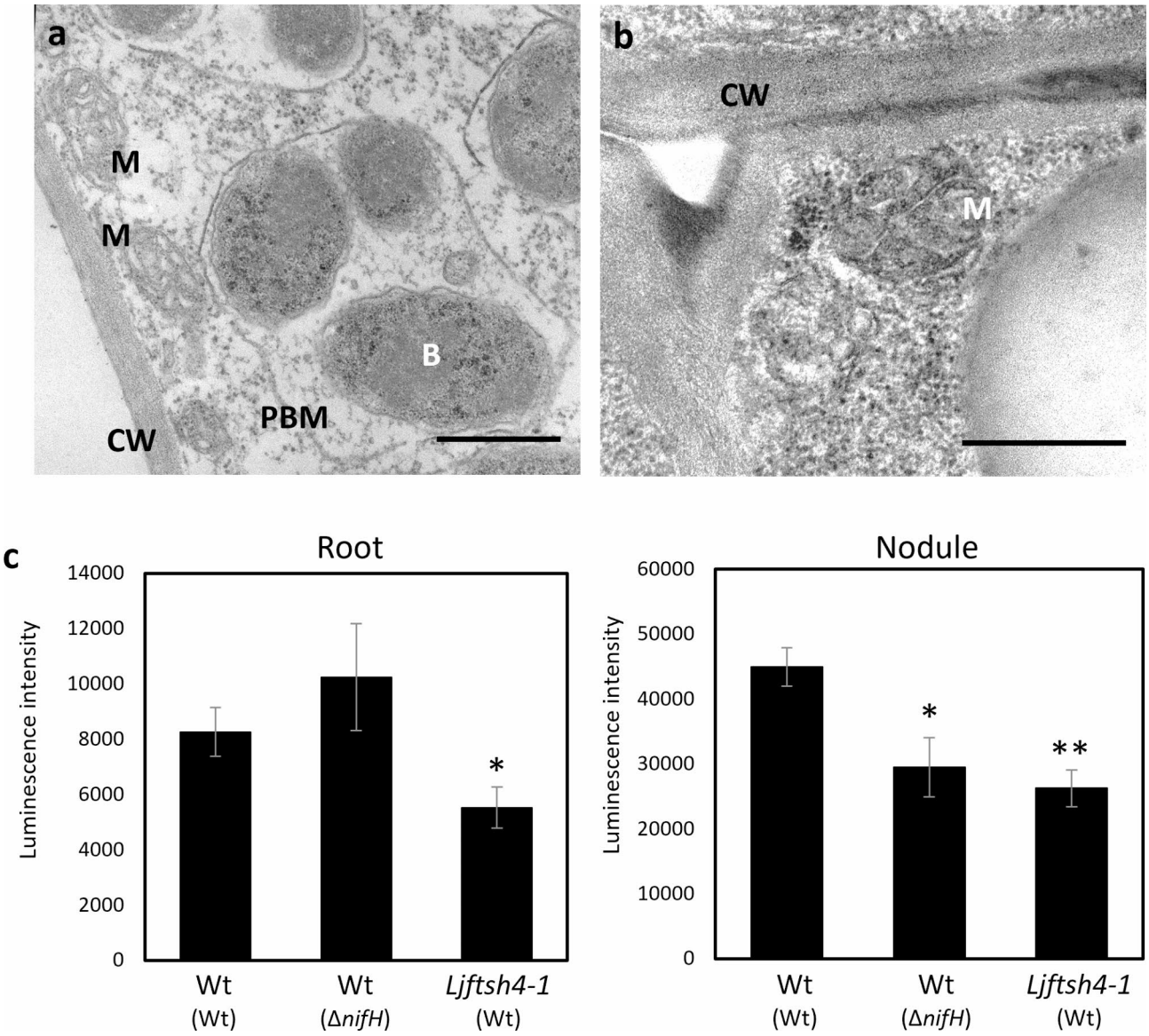

Fig. 7. Ultrastructure of nodule-infected cells and ATP contents of the wild-type and the *Ljftsh4-1* mutant. (**a**) and (**b**) TEM micrographs of nodule-infected cells of the wild-type (B-129) (**a**) and the *Ljftsh4-1* mutant (**b**) at 11 dai. B: Bacteroid, CW: cell wall, M: mitochondria. Scale bars = 0.5 µm. (**c**) ATP contents of roots and nodules of the wild-type (Wt) and the *Ljftsh4-1* mutant estimated by luminescence intensity of luciferase at 100 ms integration time. Genotypes of inoculated rhizobia are indicated in parentheses. Values are means with standard error of three independent experiments. Asterisks indicate significant differences relative to the Wt (** $P < 0.01$, * $P < 0.05$, *t*-test).

ATP and reactive oxygen species levels in *Ljfsth4* mutant

Symbiotic nitrogen fixation in root nodules requires ATP energy[55]. To determine whether the symbiotic nitrogen fixation defect in *Ljfsth4* mutants is related to ATP levels, we measured ATP content in roots and nodules using a bioluminescence assay. The root ATP content of the *Ljfsth4-1* mutant was significantly lower than that of the wild-type. In contrast, the root ATP content of wild-type plants inoculated with the nifH mutant of *M. loti* (ΔnifH) was comparable to that of wild-type plants inoculated with wild-type *M. loti* (Fig. 7c). Luminescence intensity was higher in nodules than in roots, indicating a higher ATP content in nodules. The nodule ATP content of the *Ljfsth4-1* mutant was significantly lower than that of the wild-type, similar to that of wild-type plants inoculated with the nifH mutant (Fig. 7c).

Previous studies have reported increased levels of reactive oxygen species (ROS) in *ftsh4* mutants compared to wild-type plants[56–58]. A comparison of hydrogen peroxide (H_2O_2) and superoxide (O_2^-) levels in nodules showed similar ROS generation in both wild-type and *Ljfsth4-1* mutants (Supplemental Fig. 9).

Discussion

FtsH proteases play a crucial role in the quality control of membrane proteins in bacteria and organelles of bacterial origin, such as mitochondria and chloroplasts[29]. They degrade damaged or unassembled proteins and facilitate the maturation of unfolded proteins as molecular chaperones. The plant FtsH protease family consists of multiple members, each with specific roles and localizations within the cells[48,59,60]. In *Arabidopsis*, 12 genes encoding FtsH proteases have been identified, including four in mitochondria: m-AAA (matrix) (FtsH3 and FtsH10) and i-AAA (intermembrane space) protease (FtsH4 and FtsH11)[59,61]. Phylogenetic analysis shows that LjFtsH4 is a single gene in the FtsH4 clade and is closely related to orthologs in other legumes (Fig. 3). Complementation analysis demonstrated equivalent function and activity between AtFtsH4 and LjFtsH4 (Fig. 5).

In *Arabidopsis*, loss of the FtsH4 protease causes alterations in leaf and root development under specific conditions[56]. The *Atftsh4* mutant exhibits abnormal leaf morphology in the later stages of rosette development under short-day conditions (8 h light) but not under long-day conditions (16 h light)[56]. Continuous heat stress (30 °C) under long-day conditions also halts shoot and root growth[62,63]. These developmental changes correlate with increased ROS generation and accumulation of carbonylated proteins[56]. In the case of the *ftsh4* mutant of *L. japonicus*, a Fix$^-$ phenotype was observed under normal growth conditions (16 h light, 25 °C/8 h dark, 23 °C). Additionally, no clear increase in ROS levels was observed in the nodules of the *Ljftsh4* mutants (Supplemental Fig. 9). It remains unclear whether these differences are due to species variation or distinct mechanisms of FtsH4 protease action in each plant. The *Ljftsh4* mutants showed reduced shoot growth even in the presence of sufficient nitrogen nutrition (Supplemental Figs. 1 and 4). However, it is obvious that the stunted shoot growth does not cause the Fix$^-$ phenotype of the *Ljftsh4* mutant. Grafting experiments demonstrated that nitrogen fixation activity is determined by the root genotype (Supplemental Fig. 7) and molecular transfection of *LjFtsH4* cDNA into the *Ljftsh4* mutant roots via hairy roots transformation could restore nitrogen-fixing nodule formation (Fig. 5).

Among the Fix$^-$ genes identified in *L. japonicus*, *Sst1*, *Fen1*, *Sen1*, and *Apn1* are predominantly expressed in nodules, and their expression levels increase during nodule development[18,22,33,64]. These Fix$^-$ gene mutants exhibited stunted shoot growth upon rhizobial inoculation, but under non-symbiotic conditions with sufficient nitrogen nutrition, their growth was comparable to that of the wild-type[33,65]. In contrast, *LjFtsH4* was constitutively expressed in various plant organs (Fig. 4), and *Ljftsh4* mutants exhibited reduced shoot growth, even with sufficient nitrogen nutrition (Supplemental Figs. 1 and 4). These unique features of the *LjFtsH4* set itself apart from other Fix$^-$ genes and suggest that LjFtsH4 functions not only in nodule nitrogen fixation but also in plant growth. Despite the pleiotropic functions of the LjFtsH4 being predicted, the primary phenotype of *Ljftsh4* mutants appears in nodule nitrogen fixation, highlighting the exceptional importance of LjFtsH4 in this process. The most notable feature of the *Ljftsh4* mutant is the rarity of mitochondria with normal ultrastructure in nodule cells. Unlike wild-type nodules, the folded cristae structure of mitochondria was not clearly observed in the *Ljftsh4* mutant (Fig. 7). The leaves of 14-week-old *ftsh4* mutant of *Arabidopsis* also showed similar mitochondrial ultrastructure alterations[56]. LjFtsH4 is a mitochondrial protein (Fig. 6), and thus the observed abnormalities in the mitochondria of the *Ljftsh4* mutant may be due to the loss of FtsH4 function, leading to impaired mitochondrial function. Nodule-infected cells contain numerous mitochondria, which can produce ATP more efficiently at low O_2 levels and develop characteristic metabolic capacities than mitochondria in roots and other tissues[66–68]. These cells have a high energy demand to support large supply of carbon substrate to endosymbiotic rhizobia, assimilation of the fixed nitrogen, material transport processes, and leghaemoglobin synthesis, with energy provided by nodule mitochondria[67]. Therefore, mitochondria in nodule infected cells must be highly efficient to support the substantial energy demand for nitrogen fixation as compared to those in nonsymbiotic organs. The *Ljftsh4* mutant exhibits mitochondrial abnormalities that can lead to decreased ATP levels in nodules (Fig. 7), as reported in the *Atftsh4* mutant[62]. It is likely that the decreased ATP levels in the *Ljftsh4* mutant are barely sufficient to sustain plant growth but are inadequate to support nitrogen fixation in nodules, which requires large amounts of ATP.

The nodule cells of the *Ljftsh4* mutant display senescence-like symptoms, including reduced bacteroid density and disintegration of the symbiosome membrane (Fig. 2). These phenotypes are more or less common to various Fix$^-$ mutants, but the mechanisms that trigger the breakdown of symbiosis are thought to differ depending on the function of each Fix$^-$ gene. In *Arabidopsis*, FtsH4 has been suggested to plays a role in leaf senescence as a negative regulator of plant immunity[69]. Leaf senescence and plant immunity are known to interplay with each other, and there are also some similarities in physiological responses between leaf senescence and nodule senescence[28,70]. The interplay between immunity against endosymbionts and nodule senescence has been investigated in detail in several *Medicago* Fix$^-$ mutants[28]. These studies indicate that LjFtsH4 might play a role in maintaining nitrogen-fixing activity by regulating the immune response to endosymbionts in the nodules. Transcriptome analysis of *Ljftsh4* mutant nodules could reveal the physiological responses occurring in *Ljftsh4* nodules.

Nodules produce high levels of ROS, such as superoxide radicals (O_2^-) and hydrogen peroxide (H_2O_2), due to increased respiration rates in bacteroids and mitochondria[71]. Consistent with previous studies[72–74], we detected the generation of O_2^- and H_2O_2 in young nodules, with higher amounts than in the surrounding roots (Supplemental Fig. 9). However, there were no clear differences in O_2^- and H_2O_2 levels between wild-type and *Ljftsh4-1* mutant nodules, indicating that ROS production is not the cause of the Fix$^-$ phenotype of the *Ljftsh4-1* mutant. Previous studies have reported a relationship between nodule senescence and elevated ROS production in old nodules or nodules of host plant gene-deficient mutants, such as *nad1* of *M. truncatula* and Lbs knockout mutants of *L. japonicus*[74–76]. The lack of elevated ROS in the *Ljftsh4* mutant may indicate that the senescence process of this mutant is fundamentally different from that of old nodules or nodules of host plant gene-deficient mutants.

In the MEROPS peptidase database, FtsH is classified in the metallopeptidase family[77]. Several metalloproteases have been reported to be involved in legume-rhizobium symbiosis. MtMMPL1, a metalloproteinase of *M. truncatula*, is induced in roots inoculated with symbiotic rhizobia and is proposed to be involved in the rhizobial infection process[78]. On the bacterial side, two metalloproteases of *Sinorhizobium*, HrrP and SapA, are involved in symbiotic compatibility by degrading host-derived cysteine-rich peptides (NCRs)[37,79]. These metalloproteases differ structurally and functionally from FtsH proteases. The complementation experiment using mutated LjFtsH4 variants showed that the protease activity of LjFtsH4 is necessary for its function in nodule nitrogen fixation (Supplemental Fig. 6). In *Arabidopsis*, several mitochondrial proteins have been identified as proteolytic substrates of AtFtsH4[49]. A mitochondrial small heat shock protein (HSP), HSP23.6, was identified as a proteolytic substrate of AtFtsH4, and the accumulation of HSP23.6 as the insoluble aggregated form was observed in the *Atftsh4* mutant[80]. Chungopast et al.[81] reported that the gene encoding a small heat shock protein of *L. japonicus* (chr3.CM0127.770.r2.d), similar to AtHSP23.6, was expressed in nodules and upregulated in the senescence stage. Although the function of HSP23.6 in nodules is currently unknown, FtsH4 might be involved in maintaining nodule activity by preventing the aggregation of HSP23.6. Investigating the relationship between LjFtsH4 and HSP23.6 will clarify their roles in nodule nitrogen fixation. Additionally, comparative proteomics of mitochondria between wild-type and *Ljftsh4* mutant nodules will help identify other potential counterparts of LjFtsH4, clarifying its biochemical function in symbiotic nitrogen fixation.

Understanding the roles and regulation of proteases in symbiotic nitrogen fixation is crucial for unravelling the intricate molecular mechanisms underlying this process. Further research on proteases in legume nodules can provide insights into their specific functions, interactions with other proteins, and potential applications in improving nitrogen fixation efficiency and legume crop productivity.

Materials and methods

Plant and microbial materials

The *Ljftsh4-1* mutant (G00496-9-6) was isolated from somatic mutations through intensive culture of calli and/or suspension cells of *L. japonicus* B-129 Gifu[82] plants transformed with a nodule-specific gene. The *Ljftsh4-1* mutant line was established by eliminating the transgene through segregation after backcrossing with wild-type Gifu plants. Other *Ljftsh4* mutant alleles were identified from *L. japonicus* MG-20[39] generated by C_6^+ ion beam (*Ljftsh4-2*, *Ljftsh4-3*, and *Ljftsh4-4*) or EMS (*Ljftsh4-5*). *M. loti* strain TONO[83] was used as the microsymbiont. RFP-expressing *M. loti* strain TONO[34] was used to monitor rhizobial infection inside nodules. *M. loti* was grown in tryptone-yeast extract (TY) medium containing phosphomycin (100 µg/mL) at 28 ˚C.

Phenotypic analyses

L. japonicus seeds were scarified with sandpaper and sterilized in a 5% NaOCl solution containing 0.02% Tween 20 for 10 min. After several washes with sterilized water, seeds were germinated on 0.8% agar plates in the dark. The seedlings were then transplanted into vermiculite pots supplied with nitrogen-free B&D medium[84] and grown in a growth chamber under a 16-hour day/8-hour night cycle at 25 ˚C/23 ˚C. For nodulation assays, *M. loti* was inoculated at 7 days after transplanting. Nitrogen fixation activity was analysed using an acetylene reduction assay as described in Yamaya-Ito et al.[33].

Map-based cloning

Map-based cloning of the causal gene in the *Ljftsh4-1* mutant was performed as described in Yamaya-Ito et al.[33]. The *Ljftsh4-1* mutant was crossed with *L. japonicus* ecotype MG-20. Genetic linkage analysis was conducted with SSR markers using 1644 F2 progenies. The *LjFtsH4* gene locus was mapped to a 180 kb region between the markers BM2176 and TM0349. To cover this region, *Lotus* BAC/TAC clones were selected, and ORFs on the clones were predicted using TBlastN and ORF sequences from the syntenic region of the soybean genome. Sequence comparisons of predicted ORFs between *Ljftsh4-1* mutant and wild-type genomes identified the mutation position.

The *Ljftsh4* mutant alleles derived from ecotype MG-20 were identified through genetic mapping using ecotype Gifu as a crossing partner. Fix^- lines with the mutated gene mapped close to the LjFtsH4 locus were crossed with each other to confirm that they are genetically identical alleles of the gene. Each allele was subsequently sequenced to confirm the LjFtsH4 mutation.

Plasmid constructions

For complementation of the *Ljftsh4* mutant, the full-length protein-coding region of *LjFtsH4* was amplified by PCR from cDNA synthesized from total RNA of mature plants. The amplified fragment was then cloned into the pENTR-D-TOPO vector (Invitrogen), and the resulting entry clone (ENT_LjFtsH4) was confirmed by sequencing to ensure no PCR errors. The insert from the entry clone was transferred to a Gateway-compatible binary vector, pUbi-GW-GFP[52], using an LR recombinase (Invitrogen) reaction. Point mutations in *LjFtsH4* were introduced using a PrimeSTAR mutagenesis kit (TAKARA Bio) with ENT_LjFtsH4 as the PCR template. Full-length *AtFtsH4* was amplified by PCR from cDNA synthesized from total RNA of *Arabidopsis* Col-0 seedlings and cloned into pUbi-GW-GFP using the same procedures as above.

For subcellular localization analysis of LjFtsH4, the full-length *LjFtsH4* without a stop codon was cloned into the pENTR-D-TOPO vector (Invitrogen). The insert from the entry clone was then transferred into the pK7FWG2 vector[85] to create a C-terminal GFP fusion of LjFtsH4 (LjFtsH4-GFP). The entire region of LjFtsH4-GFP was amplified by PCR and inserted between the Xba I and Kpn I sites of pUb-Hyg[52] using the In-fusion cloning system (TAKARA Bio). As a mitochondria marker, the N-terminal region (1-72aa) of the F1F0 ATPase gamma subunit of *Arabidopsis* (pFAγ, AT2G33040) was amplified by PCR from cDNA synthesized from total RNA of *Arabidopsis* (Col-0) seedlings. The amplified fragment was connected with PCR-amplified RFP to create

pFAγ-RFP and cloned into pUb-Hyg. LjFtsH4-GFP and pFAγ-RFP were then transformed into *Agrobacterium rhizogenes* LBA1334 and AR1193, respectively, and used for hairy root transformation. Primers used for plasmid constructions are listed in Supplemental Table 1.

Hairy root transformation

Hairy root transformation was performed according to the procedures described by Shimoda et al.[86], using *A. rhizogenes* LBA1334[87]. Plants with GFP-positive hairy roots were transplanted into vermiculite supplemented with B&D medium containing 0.5 mM ammonium nitrate. For nodulation, *M. loti* strain TONO was inoculated at 5 days after transplanting, and the plants were grown in a growth chamber with a 16-hour light/8-hour dark cycle at 25 ˚C/23 ˚C. The nodulation phenotype was examined using an MZFLIII stereomicroscope (Leica).

Light and electron microscopy

The nodules were fixed in 4.0% paraformaldehyde and 2.5% glutaraldehyde in 0.1 M sodium phosphate buffer (pH 7.0) for 3 h and then overnight at 4 ˚C. After several washes with the same buffer, the samples were post-fixed in 2.0% osmium tetroxide in the same buffer for 3–4 h at room temperature. They were dehydrated through graded ethanol and acetone series and finally embedded in epoxy resin (Quetol-812, Nisshin EM Co. Ltd., Tokyo, Japan). Thin sections (~ 1 μm) for light microscopy and ultrathin sections (~ 0.05 μm) for electron microscopy were made using an ultramicrotome (Ultra Cut-R, Leica Microsystems). Thin sections were placed on a slide glass, stained with 0.002% (w/v) toluidine blue, and observed with an optical microscope. Ultrathin sections were stained with uranium acetate and lead citrate for observation using an electron microscope (H-700, Hitachi, Tokyo, Japan).

Gene expression analysis

Total RNAs were isolated using the cetyl trimethyl ammonium bromide (CTAB) method, followed by purification with the RNeasy Plant Mini Kit (QIAGEN)[33]. cDNA synthesis was performed using the Quantitect Reverse Transcriptase Kit (QIAGEN) and quantitative RT-PCR (qRT-PCR) was conducted on the Light Cycler 2.0 (Roche) with FastStart DNA Master SYBR Green I (Roche), following the manufacturer's instructions. *L. japonicus* ubiquitin (LjUbq)[88] was used as internal standard. Primers used for qRT-PCR are listed in Supplemental Table 1.

Measurement of ATP content

The wild-type and *Ljftsh4* mutants were grown as described above (see phenotypic analyses). Fourteen days post-inoculation with *M. loti*, nodules were detached from roots and frozen in liquid nitrogen. The frozen nodules and nodule-detached roots were ground using a RETSCH MM300 TissueLyser Mill Mixer (QIAGEN) with zirconia balls. ATP extraction was performed according to Hou et al.[89]. 500 µl of 50 mM Tris-HCl buffer (pH 7.4) was added to 100 mg samples and incubated at 95 °C for 10 min. After centrifugation (15,000 rpm at 4 °C for 10 min), the supernatant was collected and 100 µL aliquots were stored at − 80 °C until ATP measurement. ATP content was measured using the Tissue ATP Assay Kit (WAKO, CatNo. 302-31801), which detects ATP based on the luciferin-luciferase assay method. Luminescence intensity was measured using an Infinite M1000 Pro plate reader (Tecan).

Computer analysis

Functional domains of LjFtsH4 were analysed using InterProScan[41]. Subcellular localization was predicted using TargetP[50] and MultiLOC[51]. Phylogenetic analysis of FtsH4 was performed using the Phylogeny.fr platform[90].

Data availability

All data generated or analyzed during this study are included in this published article and in its Supplementary material.

Received: 4 September 2024; Accepted: 29 October 2024
Published online: 11 November 2024

References

1. Radutoiu, S. et al. Plant recognition of symbiotic bacteria requires two LysM receptor-like kinases. *Nature*. **425**, 585–592 (2003).
2. Madsen, E. B. et al. A receptor kinase gene of the LysM type is involved in legume perception of rhizobial signals. *Nature*. **425**, 637–640 (2003).
3. Limpens, E. et al. LysM domain receptor kinases regulating rhizobial nod factor-induced infection. *Science*. **302**, 630–633 (2003).
4. Jhu, M. Y. & Oldroyd, G. E. D. Dancing to a different tune, can we switch from chemical to biological nitrogen fixation for sustainable food security? *PLoS Biol.* **21**, e3001982 (2023).
5. Imaizumi-Anraku, H. et al. Plastid proteins crucial for symbiotic fungal and bacterial entry into plant roots. *Nature*. **433**, 527–531 (2005).
6. Ane, J. M. et al. *Medicago truncatula* DMI1 required for bacterial and fungal symbioses in legumes. *Science*. **303**, 1364–1367 (2004).
7. Charpentier, M. et al. Nuclear-localized cyclic nucleotide-gated channels mediate symbiotic calcium oscillations. *Science*. **352**, 1102–1105 (2016).
8. Capoen, W. et al. Nuclear membranes control symbiotic calcium signaling of legumes. *Proc. Natl. Acad. Sci. USA*. **108**, 14348–14353 (2011).
9. Kanamori, N. et al. A nucleoporin is required for induction of Ca^{2+} spiking in legume nodule development and essential for rhizobial and fungal symbiosis. *Proc. Natl. Acad. Sci. USA* **103**, 359–364 (2006).
10. Saito, K. et al. NUCLEOPORIN85 is required for calcium spiking, fungal and bacterial symbioses, and seed production in *Lotus japonicus*. *Plant. Cell.* **19**, 610–624 (2007).

11. Groth, M. et al. NENA, a *Lotus japonicus* homolog of Sect. 13, is required for rhizodermal infection by arbuscular mycorrhiza fungi and rhizobia but dispensable for cortical endosymbiotic development. *Plant. Cell.* **22**, 2509–2526 (2010).
12. Tirichine, L. et al. Deregulation of a Ca^{2+}/calmodulin-dependent kinase leads to spontaneous nodule development. *Nature*. **441**, 1153–1156 (2006).
13. Levy, J. et al. A putative Ca^{2+} and calmodulin-dependent protein kinase required for bacterial and fungal symbioses. *Science*. **303**, 1361–1364 (2004).
14. Yano, K. et al. CYCLOPS, a mediator of symbiotic intracellular accommodation. *Proc. Natl. Acad. Sci. USA*. **105**, 20540–20545 (2008).
15. Messinese, E. et al. A novel nuclear protein interacts with the symbiotic DMI3 calcium- and calmodulin-dependent protein kinase of *Medicago truncatula*. *Mol. Plant. Microbe Interact.* **20**, 912–921 (2007).
16. Soyano, T., Kouchi, H., Hirota, A. & Hayashi, M. Nodule inception directly targets NF-Y subunit genes to regulate essential processes of root nodule development in *Lotus japonicus*. *PLoS Genet.* **9**, e1003352 (2013).
17. Soyano, T., Shimoda, Y., Kawaguchi, M. & Hayashi, M. A shared gene drives lateral root development and root nodule symbiosis pathways in *Lotus*. *Science*. **366**, 1021–1023 (2019).
18. Hakoyama, T. et al. Host plant genome overcomes the lack of a bacterial gene for symbiotic nitrogen fixation. *Nature*. **462**, 514–517 (2009).
19. Ott, T. et al. Symbiotic leghemoglobins are crucial for nitrogen fixation in legume root nodules but not for general plant growth and development. *Curr. Biol.* **15**, 531–535 (2005).
20. Baier, M. C., Barsch, A., Küster, H. & Hohnjec, N. Antisense repression of the *Medicago truncatula* nodule-enhanced sucrose synthase leads to a handicapped nitrogen fixation mirrored by specific alterations in the symbiotic transcriptome and metabolome. *Plant. Physiol.* **145**, 1600–1618 (2007).
21. Nomura, M. et al. Phosphoenolpyruvate carboxylase plays a crucial role in limiting nitrogen fixation in *Lotus japonicus* nodules. *Plant. Cell. Physiol.* **47**, 613–621 (2006).
22. Krusell, L. et al. The sulfate transporter SST1 is crucial for symbiotic nitrogen fixation in *Lotus japonicus* root nodules. *Plant. Cell.* **17**, 1625–1636 (2005).
23. Chu, Q. et al. SEN1 is responsible for molybdate transport into nodule symbiosomes for nitrogen fixation in *Lotus japonicus*. 10.1101 /2022.11.10.515970v1. Preprint https://www.biorxiv.org/content/ (2022).
24. Roy, S. et al. Celebrating 20 years of genetic discoveries in legume nodulation and symbiotic nitrogen fixation. *Plant. Cell.* **32**, 15–41 (2020).
25. Mergaert, P. et al. A novel family in *Medicago truncatula* consisting of more than 300 nodule-specific genes coding for small, secreted polypeptides with conserved cysteine motifs. *Plant. Physiol.* **132**, 161–173 (2003).
26. Horváth, B. et al. Loss of the nodule-specific cysteine rich peptide, NCR169, abolishes symbiotic nitrogen fixation in the *Medicago truncatula dnf7* mutant. *Proc. Natl. Acad. Sci. USA*. **112**, 15232–15237 (2015).
27. Kim, M. et al. An antimicrobial peptide essential for bacterial survival in the nitrogen-fixing symbiosis. *Proc. Natl. Acad. Sci. USA*. **112**, 15238–15243 (2015).
28. Berrabah, F. et al. Defense and senescence interplay in legume nodules. *Plant. Commun.* **5**, 100888 (2024).
29. Janska, H., Kwasniak, M. & Szczepanowska, J. Protein quality control in organelles - AAA/FtsH story. *Biochim. Biophys. Acta*. **1833**, 381–387 (2013).
30. van Wyk, S. G., Du Plessis, M., Cullis, C. A., Kunert, K. J. & Vorster, B. J. Cysteine protease and cystatin expression and activity during soybean nodule development and senescence. *BMC Plant. Biol.* **14**, 294 (2014).
31. Pierre, O. et al. Involvement of papain and legumain proteinase in the senescence process of *Medicago truncatula* nodules. *New. Phytol.* **202**, 849–863 (2014).
32. Yang, L., Syska, C., Garcia, I., Frendo, P. & Boncompagni, E. Involvement of proteases during nodule senescence in leguminous plants. In *The Model Legume Medicago truncatula*. 1st Ed. (edited by Frans J. de Bruijn). 683–693 (2020).
33. Yamaya-Ito, H. et al. Loss-of-function of ASPARTIC PEPTIDASE NODULE-INDUCED 1 (APN1) in *Lotus japonicus* restricts efficient nitrogen-fixing symbiosis with specific *Mesorhizobium loti* strains. *Plant. J.* **93**, 5–16 (2018).
34. Shimoda, Y. et al. The rhizobial autotransporter determines the symbiotic nitrogen fixation activity of *Lotus japonicus* in a host-specific manner. *Proc. Natl. Acad. Sci. USA*. **117**, 1806–1815 (2020).
35. Van de Velde, W. et al. Plant peptides govern terminal differentiation of bacteria in symbiosis. *Science*. **327**, 1122–1126 (2010).
36. Wang, D. et al. A nodule-specific protein secretory pathway required for nitrogen-fixing symbiosis. *Science*. **327**, 1126–1129 (2010).
37. Price, P. A. et al. Rhizobial peptidase HrrP cleaves host-encoded signaling peptides and mediates symbiotic compatibility. *Proc. Natl. Acad. Sci. USA* **112**, 15244–15249 (2015).
38. Sandal, N. et al. Genetics of symbiosis in *Lotus japonicus*: recombinant inbred lines, comparative genetic maps, and map position of 35 symbiotic loci. *Mol. Plant. Microbe Interact.* **19**, 80–91 (2006).
39. Kawaguchi, M. *Lotus japonicus* 'Miyakojima' MG-20: An early-flowering accession suitable for indoor handling. *J. Plant. Res.* **113**, 507–509 (2000).
40. Sato, S. et al. Genome structure of the legume, *Lotus japonicus*. *DNA Res.* **15**, 227–239 (2008).
41. Jones, P. et al. InterProScan 5: Genome-scale protein function classification. *Bioinformatics*. **30**, 1236–1240 (2014).
42. Thorsness, P. E., White, K. H. & Fox, T. D. Inactivation of YME1, a member of the ftsH-SEC18-PAS1-CDC48 family of putative ATPase-encoding genes, causes increased escape of DNA from mitochondria in *Saccharomyces cerevisiae*. *Mol. Cell. Biol.* **13**, 5418–5426 (1993).
43. Urantowka, A., Knorpp, C., Olczak, T., Kolodziejczak, M. & Janska, H. Plant mitochondria contain at least two *i*-AAA-like complexes. *Plant. Mol. Biol.* **59**, 239–252 (2005).
44. Chen, J., Burke, J. J., Velten, J. & Xin, Z. FtsH11 protease plays a critical role in *Arabidopsis* thermotolerance. *Plant. J.* **48**, 73–84 (2006).
45. Benedito, V. A. et al. A gene expression atlas of the model legume *Medicago truncatula*. *Plant. J.* **55**, 504–513 (2008).
46. Karata, K., Inagawa, T., Wilkinson, A. J., Tatsuta, T. & Ogura, T. Dissecting the role of a conserved motif (the second region of homology) in the AAA family of ATPases. Site-directed mutagenesis of the ATP-dependent protease FtsH. *J. Biol. Chem.* **74**, 26225–26232 (1999).
47. Saikawa, N., Ito, K. & Akiyama, Y. Identification of glutamic acid 479 as the gluzincin coordinator of zinc in FtsH (HflB). *Biochemistry*. **41**, 1861–1868 (2002).
48. Shan, Q. et al. Genome-wide identification and comprehensive analysis of the *FtsH* gene family in soybean (*Glycine max*). *Int. J. Mol. Sci.* **24**, 16996 (2023).
49. Opalińska, M., Parys, K. & Jańska, H. Identification of physiological substrates and binding partners of the plant mitochondrial protease FTSH4 by the trapping approach. *Int. J. Mol. Sci.* **18**, 2455 (2017).
50. Emanuelsson, O., Nielsen, H., Brunak, S. & von Heijne, G. Predicting subcellular localization of proteins based on their N-terminal amino acid sequence. *J. Mol. Biol.* **300**, 1005–1016 (2000).
51. Höglund, A., Dönnes, P., Blum, T., Adolph, H. W. & Kohlbacher, O. MultiLoc: Prediction of protein subcellular localization using N-terminal targeting sequences, sequence motifs and amino acid composition. *Bioinformatics*. **22**, 1158–1165 (2006).
52. Maekawa, T. et al. Polyubiquitin promoter-based binary vectors for overexpression and gene silencing in *Lotus japonicus*. *Mol. Plant. Microbe Interact.* **21**, 375–382 (2008).

53. Lee, S. et al. Mitochondrial targeting of the *Arabidopsis* F1-ATPase γ-subunit via multiple compensatory and synergistic presequence motifs. *Plant. Cell.* **24**, 5037–5057 (2012).
54. Joubert, F. & Puff, N. Mitochondrial cristae architecture and functions: Lessons from minimal model systems. *Membranes*. **11**, 465 (2021).
55. Threatt, S. D. & Rees, D. C. Biological nitrogen fixation in theory, practice, and reality: A perspective on the molybdenum nitrogenase system. *FEBS Lett.* **597**, 45–58 (2023).
56. Gibala, M. et al. The lack of mitochondrial AtFtsH4 protease alters *Arabidopsis* leaf morphology at the late stage of rosette development under short-day photoperiod. *Plant. J.* **59**, 685–699 (2009).
57. Dolzblasz, A. et al. The mitochondrial protease AtFTSH4 safeguards *Arabidopsis* shoot apical meristem function. *Sci. Rep.* **6**, 28315 (2016).
58. Hong, L. et al. Variable cell growth yields reproducible organ development through spatiotemporal averaging. *Dev. Cell.* **38**, 15–32 (2016).
59. Yu, F., Park, S. & Rodermel, S. R. The *Arabidopsis* FtsH metalloprotease gene family: interchangeability of subunits in chloroplast oligomeric complexes. *Plant. J.* **37**, 864–786 (2004).
60. Zhu, X. et al. Genome-wide identification and characterization of filamentation temperature-sensitive H (FtsH) genes and expression analysis in response to multiple stresses in *Medicago truncatula*. *Mol. Biol. Rep.* **50**, 10097–10109 (2023).
61. Opalińska, M.& Jańska, H. A. A. A. Proteases guardians mitochondrial function homeost. *Cells* **7**, 163 (2018).
62. Smakowska, E. et al. Lack of FTSH4 protease affects protein carbonylation, mitochondrial morphology, and phospholipid content in mitochondria of *Arabidopsis*: New insights into a complex interplay. *Plant. Physiol.* **171**, 2516–2535 (2016).
63. Dolzblasz, A. et al. Impairment of meristem proliferation in plants lacking the mitochondrial protease AtFTSH4. *Int. J. Mol. Sci.* **19**, 853 (2018).
64. Hakoyama, T. et al. The integral membrane protein SEN1 is required for symbiotic nitrogen fixation in *Lotus japonicus* nodules. *Plant. Cell. Physiol.* **53**, 225–236 (2012).
65. Kumagai, H. et al. A novel ankyrin-repeat membrane protein, IGN1, is required for persistence of nitrogen-fixing symbiosis in root nodules of *Lotus japonicus*. *Plant. Physiol.* **143**, 1293–1305 (2007).
66. Millar, A. H., Day, D. A. & Bergersen, F. J. Microaerobic respiration and oxidative phosphorylation by soybean nodule mitochondria: Implications for nitrogen fixation. *Plant. Cell. Environ.* **18**, 715–726 (1995).
67. Booth, N. J., Smith, P. M. C., Ramesh, S. A. & Day, D. A. Malate transport and metabolism in nitrogen-fixing legume nodules. *Molecules*. **26**, 6876 (2021).
68. Sin, W. C., Liu, J., Zhong, J. Y., Lam, H. M. & Lim, B. L. Comparative proteomics analysis of root and nodule mitochondria of soybean. *Plant Cell Environ*. (**in press**) (2024).
69. Zhang, S. et al. The *Arabidopsis* mitochondrial protease FtSH4 is involved in leaf senescence via regulation of WRKY-dependent salicylic acid accumulation and signaling. *Plant. Physiol.* **173**, 2294–2307 (2017).
70. Zhang, Y., Wang, H. L., Li, Z. & Guo, H. Genetic network between leaf senescence and plant immunity: Crucial regulatory nodes and new insights. *Plants*. **9**, 495 (2020).
71. Matamoros, M. A. et al. Mitochondria are an early target of oxidative modifications in senescing legume nodules. *New. Phytol*. **197**, 873–885 (2013).
72. Santos, R., Hérouart, D., Sigaud, S., Touati, D. & Puppo, A. Oxidative burst in alfalfa-*Sinorhizobium meliloti* symbiotic interaction. *Mol. Plant. Microbe Interact.* **14**, 86–89 (2001).
73. Chen, D. S. et al. Identification of a core set of rhizobial infection genes using data from single cell-types. *Front. Plant. Sci.* **6**, 575 (2015).
74. Wang, C. et al. NODULES WITH ACTIVATED DEFENSE 1 is required for maintenance of rhizobial endosymbiosis in *Medicago truncatula*. *New. Phytol.* **212**, 176–191 (2016).
75. Montiel, J., Arthikala, M. K., Cárdenas, L. & Quinto, C. Legume NADPH oxidases have crucial roles at different stages of nodulation. *Int. J. Mol. Sci.* **17**, 680 (2016).
76. Wang, L. et al. CRISPR/Cas9 knockout of leghemoglobin genes in *Lotus japonicus* uncovers their synergistic roles in symbiotic nitrogen fixation. *New. Phytol.* **224**, 818–832 (2019).
77. Rawlings, N. D. et al. The MEROPS database of proteolytic enzymes, their substrates and inhibitors in 2017 and a comparison with peptidases in the PANTHER database. *Nucleic Acids Res.* **46**, D624–D632 (2018).
78. Combier, J. P. et al. The MtMMPL1 early nodulin is a novel member of the matrix metalloendoproteinase family with a role in *Medicago truncatula* infection by *Sinorhizobium meliloti*. *Plant. Physiol.* **144**, 703–716 (2007).
79. Benedict, A. B., Ghosh, P., Scott, S. M. & Griffitts, J. S. A conserved rhizobial peptidase that interacts with host-derived symbiotic peptides. *Sci. Rep.* **11**, 11779 (2021).
80. Maziak, A., Heidorn-Czarna, M., Weremczuk, A. & Janska, H. FTSH4 and OMA1 mitochondrial proteases reduce moderate heat stress-induced protein aggregation. *Plant. Physiol.* **187**, 769–786 (2021).
81. Chungopast, S. et al. Transcriptomic profiles of nodule senescence in *Lotus japonicus* and *Mesorhizobium loti* symbiosis. *Plant. Biotech.* **31**, 345–349 (2014).
82. Handberg, K. & Stougaard, J. *Lotus japonicus*, an autogamous, diploid legume species for classical and molecular genetics. *Plant. J.* **2**, 487–496 (1992).
83. Kawaguchi, M. et al. Root, root hair, and symbiotic mutants of the model legume *Lotus japonicus*. *Mol. Plant. Microbe Interact.* **15**, 17–26 (2002).
84. Broughton, W. J. & Dilworth, M. J. Control of leghaemoglobin synthesis in snake beans. *Biochem. J.* **125**, 1075–1080 (1971).
85. Karimi, M., Inzé, D. & Depicker, A. GATEWAY™ vectors for *Agrobacterium*-mediated plant transformation. *Trends Plant. Sci.* **7**, 193–195 (2002).
86. Shimoda, Y. et al. Rhizobial and fungal symbioses show different requirements for calmodulin binding to calcium calmodulin-dependent protein kinase in *Lotus japonicus*. *Plant. Cell.* **24**, 304–321 (2012).
87. Offringa, I. A. et al. Complementation of *Agrobacterium tumefaciens* tumor-inducing aux mutants by genes from the T(R)-region of the Ri plasmid of *Agrobacterium rhizogenes*. *Proc. Natl. Acad. Sci. USA* **83**, 6935–6939 (1986).
88. Flemetakis, E. et al. *Lotus japonicus* contains two distinct ENOD40 genes that are expressed in symbiotic, nonsymbiotic, and embryonic tissues. *Mol. Plant. Microbe Interact.* **13**, 987–994 (2000).
89. Hou, Q. Z. et al. The responses of photosystem II and intracellular ATP production of *Arabidopsis* leaves to salt stress are affected by extracellular ATP. *J. Plant. Res.* **131**, 331–339 (2018).
90. Dereeper, A. et al. Phylogeny.fr: Robust phylogenetic analysis for the non-specialist. *Nucleic Acids Res.* **36**, W465–469 (2008).

Acknowledgements

The authors are grateful to Yoshihiro Hase and Atsushi Tanaka for C_6^+ ion beam irradiation of *L. japonicus* seeds, and Fumiko Yukuhiro and Kenji Watanabe for their help with electron microscopy. The seeds of *L. japonicus* B-129 and MG-20 were obtained from the National BioResource Project *Lotus* and *Glycine* with permission

to collect plants. This work was supported by Japan Society for the Promotion of Science KAKENHI grants to Y.U. (Grant No. 17570044) and Y.S. (Grant No. 21K05335), as well as the JST Mirai Program (Grant No. JPMJMI20E4) to S.S. and Y.S.

Author contributions

Y.S., H.Y.-I., H.K., and Y.U. designed the research; Y.S. and H.Y.-I. performed experiments and analysed data with support from T.H., S.S., M.H., H.K., and Y.U.; S.S., M.K., N.S., and Y.U. identified the mutant; S.S., T.K., and Y.U. identified the causal gene of the mutant; Y.S. and H.Y.-I. wrote the paper with help from all the authors.

Declarations

Competing interests

The authors declare no competing interests.

Additional information

Supplementary Information The online version contains supplementary material available at https://doi.org/10.1038/s41598-024-78295-5.

Correspondence and requests for materials should be addressed to Y.S. or Y.U.

Reprints and permissions information is available at www.nature.com/reprints.

Publisher's note Springer Nature remains neutral with regard to jurisdictional claims in published maps and institutional affiliations.